

Comparative Analysis of AlN Thin Film Uniformity on 2-Inch and 4-Inch Si Wafers Prepared by Magnetron Sputtering

Zulkifli Azman¹, Falah Abid Mohammad Shuhaili¹, Ahmad Shuhaimi Abu Bakar², Mohd Rofei Mat Husin³, Jahanzeb Khan⁴, Nafarizal Nayan^{5*}

¹ Faculty of Electrical and Electronic Engineering,
Universiti Tun Hussein Onn Malaysia, Batu Pahat, 86400, MALAYSIA

² Low Dimensional Material Research,
Universiti Malaya, Kuala Lumpur, 50603, MALAYSIA

³ MIMOS Semiconductor (M) Sdn Bhd,
Technology Park Malaysia, Kuala Lumpur, 57000, MALAYSIA

⁴ Electrical and Computer Engineering Department, Faculty of Engineering,
King Abdulaziz University, Jeddah, 21589, SAUDI ARABIA

⁵ Microelectronics and Nanotechnology - Shamsuddin Research Centre (MiNT-SRC),
Universiti Tun Hussein Onn Malaysia, Batu Pahat, 86400, MALAYSIA

*Corresponding Author: nafa@uthm.edu.my

DOI: <https://doi.org/10.30880/ijie.2025.17.06.016>

Article Info

Received: 30 May 2025

Accepted: 16 September 2025

Available online: 30 December 2025

Keywords

Aluminium nitride (AlN), crystalline quality, silicon wafer, RF magnetron sputtering, thin film deposition

Abstract

The uniformity of aluminium nitride (AlN) thin films produced via RF magnetron sputtering on 2-inch and 4-inch silicon (111) wafers is compared in this work. X-ray diffraction (XRD), surface profilometry, and field emission scanning electron microscopy (FESEM) were used to assess the homogeneity of the film. XRD analysis confirmed (100) orientation at $\sim 33.5^\circ$ (2θ) for both wafers belong to hexagonal wurtzite structure of AlN. The 2-inch wafer exhibited consistent peak intensity across all eight positions, while the 4-inch wafer showed weaker intensity at the edges, indicating reduced crystalline quality. Thickness measurements showed that the AlN on 2-inch wafer had a range of 133.38–168.45 nm with an average of 154.28 nm, standard deviation of 10.98 nm, and a coefficient of variation (CV) of 7.12%. In comparison, the 4-inch wafer showed a broader thickness range of 134.00–188.28 nm, with an average of 168.68 nm, standard deviation of 13.74 nm, and CV of 8.15%. FESEM images revealed uniform, compact grains across the 2-inch wafer and small grains and less compact morphology near the edges of the 4-inch wafer. The reduced uniformity in the 4-inch wafer is attributed to lower adatom mobility at the edges, due to decreased plasma density and mismatch between wafer and 3-inch target size. Overall, the 2-inch wafer demonstrated excellent film uniformity.

1. Introduction

Aluminium nitride, (AlN) a material belonging to the class of wide-bandgap semiconductors, has been characterized by high thermal conductivity, a significant dielectric constant, mechanical stability, and ultraviolet transparency, and, therefore, can be applied for increasing the efficiency of electronics,

optoelectronics, and sensor devices [1]–[4]. There are several ways of fabricating AlN thin films, including molecular beam epitaxy (MBE) [5], chemical vapour deposition (CVD) [6], and physical vapour deposition (PVD) techniques such as magnetron sputtering [7][8].

AlN thin films generally exhibit a hexagonal wurtzite structure with preferred c-axis orientation, regardless of substrate, but the degree of crystallinity and grain size varies [9]–[11]. In some way, the substrate aids in the development of high crystalline structure of AlN deposition using magnetron sputtering. According to earlier research, Silicon, (Si) has been used as a substrate on a large scale. Although several studies have found c-sapphire to be good [12]–[14], Si substrates are the greatest option in the semiconductor industry due to their cost and versatility [15]. Films on sapphire often show larger grain size and roughness, while those on Si substrate can have higher refractive indices and smoother surfaces [11][16]. A significant issue in employing AlN thin films on Si substrates is attaining uniform, high-quality deposition over extensive wafers. This challenge mostly stems from lattice mismatch, resulting in strain and flaws inside the films [17]–[19]. Critical concerns are the regulation of thickness uniformity, crystal orientation, and defect density, all of which exhibit significant sensitivity to deposition parameters and substrate characteristics

AlN films deposited on Si (111) wafers have been shown to exhibit excellent crystallinity and improved uniformity, contributing to enhanced device reliability and reduced production costs [20][21]. However, even if deposition processes have improved, keeping film characteristics consistent, especially over larger wafer surfaces, is still a big problem. Changes in the size of the substrate can affect the consistency and quality of AlN films because of uneven plasma-induced substrate heating, uneven precursor distribution, or stress relaxation mechanisms. The difference in lattice structure between AlN and Si makes this problem much worse, which could lower the films' structural, morphological, and electrical performance [22][23]. To address these challenges, this study compares AlN deposited on 2-inch and 4-inch Si wafers. The properties such as crystal structure, surface morphology, and film thickness were studied. The aim is to determine how substrate size influences the uniformity and overall quality of AlN thin films, thereby guiding future optimization for scalable device fabrication.

2. Methodology

2.1 Substrate Preparation

Si wafers with a crystal orientation of (111) with two different sizes of wafers, i.e. diameter of 2-inch and 4-inch were used as substrates. Si is chosen due to its long-established role in semiconductor manufacturing [24]. They provide a solid and stable foundation for the construction of thin material layers. Because of the atomic arrangement that smoothest the surface for further process stages, the (111) orientation is recommended [15]. A wafer n-type Si with (111) orientation with one side polished served as the foundation for this study. A 1:5 ratio solution of hydrofluoric acid (HF) and deionised water (DI) is used to clean and treat Si before the deposition process. The cleaning process is to remove the unwanted elements such as the native oxide layer that may affect the formation of epitaxial layer of AlN on the Si substrate.

2.2 Area Arrangement on Si Wafers for Uniformity Analysis

We arrange Si wafers into multiple smaller sections for our assessment of their surface uniformity. For 4-inch wafers we created 16 sections and for 2-inch wafers we created 8 sections as shown in Fig. 1. Through surface analysis approach, we evaluated different sections to verify consistent physical properties and uniformity. Reliable performance in semiconductor applications requires uniform materials because performance depends on both surface shape and crystal structure and doping concentrations [25]. The investigation of different sections allows us to detect variations which leads to a better comprehension of material distribution. This detailed analysis ensures which sections had good distribution in uniformity.

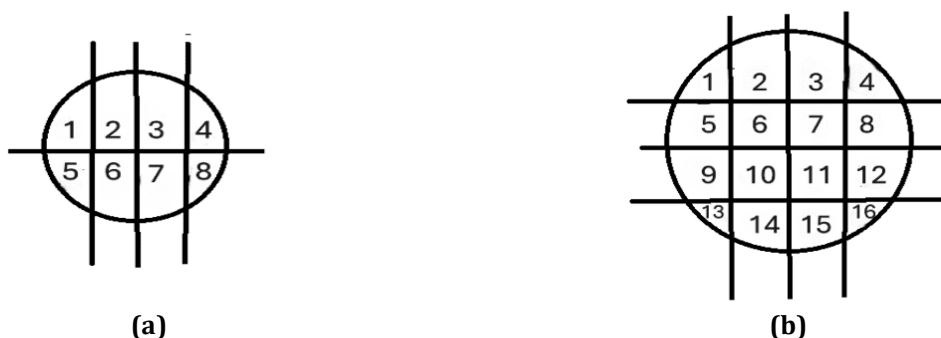


Fig. 1 Sections point on Si wafer; (a) 2-inch Si wafer for 8 sections; and (b) 4-inch Si wafer for 16 sections

2.3 Deposition of AlN Thin Film

AlN thin films were deposited using an RF magnetron sputtering system (SNTEK Korea). The process began with placing cleaned Si wafers into a sputtering chamber, which was then evacuated to a high vacuum of 7×10^{-6} Torr. A 3-inch-diameter, 1/8-inch-thick (99.998%) Aluminium, (Al) target procured from ITASCO, Korea was positioned at a 45-degree oblique angle for deposition at distance of 5-inch from substrate. The chamber is equipped with a dual-gun configuration for co-sputtering applications; however, only a single target gun was used in this study, resulting in the 45-degree oblique target orientation. For deposition, argon (Ar) and nitrogen (N₂) gases were introduced to create plasma, enabling Al atoms to sputter from the target and reacted with N₂ to form AlN films on the substrate. The sputtering pressure was set at 3 mTorr, while the Ar/N₂ gas mixture was fixed 75:50 sccm. The RF power was fixed at 300W, substrate rotation speed fixed at 10 rpm, deposition time 1 hour, for both 2-inch and 4-inch Si wafer. The deposition was carried out without any external heat supplied to the substrate. Please note that these sputtering parameters have been explained elsewhere, as they were selected to achieve the optimal conditions for producing (100) preferred orientation of AlN thin films on Si wafers at room temperature with this sputtering chamber setup [26]. Fig. 2 shows the schematic diagram of sputtering system was used in this study.

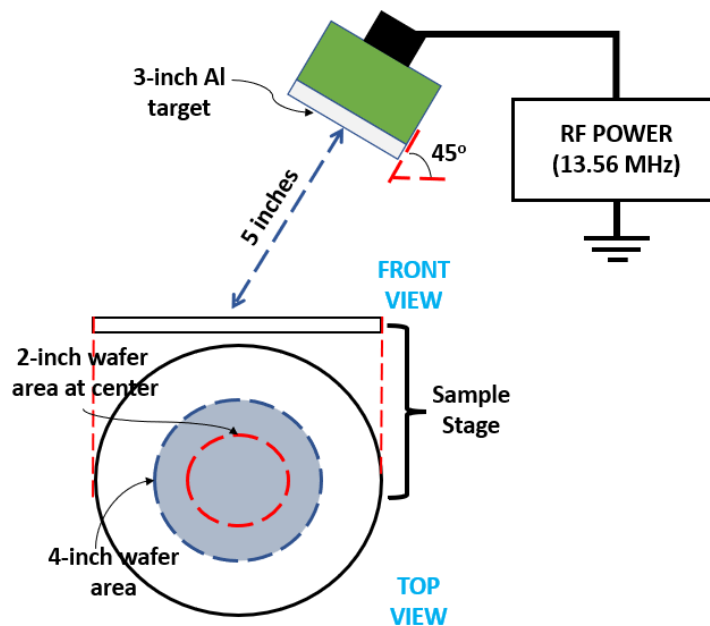


Fig.2 Schematic diagram of RF magnetron sputtering system for 2-inch and 4-inch AlN thin film deposition

2.4 Characterisations of AlN Thin Film

Several analytical instruments were employed to characterize the properties of the AlN thin films. These include a Panalytical X-ray diffractometer (XRD) for crystal structure analysis, a Bruker surface profiler for thickness measurements, and a JEOL JSM-7600F Field Emission Scanning Electron Microscope (FESEM) for surface morphology examination. X-ray diffraction was performed using a CuK α anode source with a wavelength of 1.5406 Å. The 2θ range was set from 20° to 80° with a step size of 0.03°. The generator operated at 40 kV and 40 mA, and a $\frac{1}{4}$ ° divergence slit was used. To evaluate the uniformity of the AlN films across both 2-inch and 4-inch wafers, the arithmetic Coefficient of Variation (CV) was calculated.

3. Results and Discussion

3.1 Crystal Structure of AlN Thin Film

Fig. 3 presents the X-ray diffraction (XRD) patterns of AlN thin films measured at multiple positions across both 2-inch and 4-inch silicon (Si) wafers. The dominant diffraction peak observed at approximately 33.5° (2θ) corresponds to the (100) plane of the hexagonal wurtzite AlN structure, confirming the preferential orientation of the deposited films. For the 2-inch wafer, XRD measurements were taken at eight different locations, all of which consistently exhibited the (100) peak with some variation in peak intensity and position. Similarly, for the 4-inch wafer, sixteen measurement points across the wafer also showed consistent (100) peak characteristics.

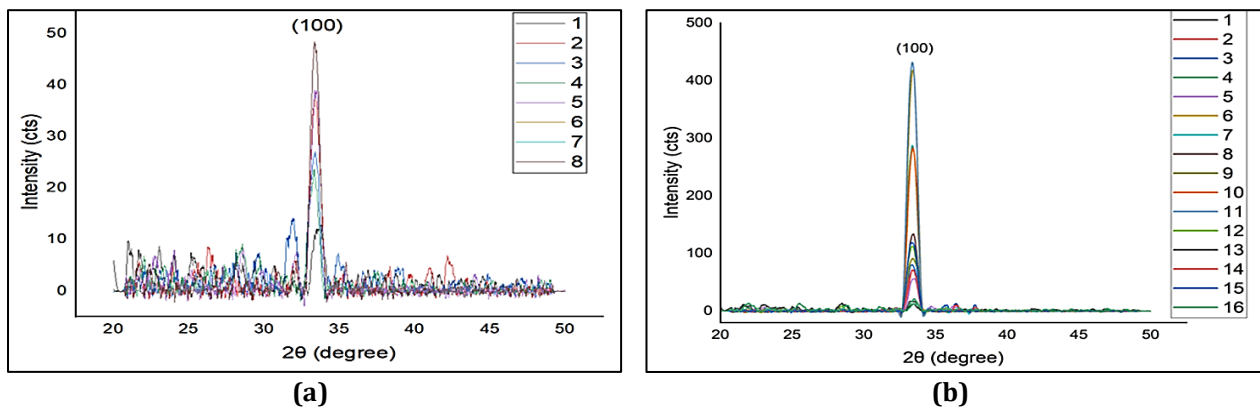


Fig.3 XRD patterns of AlN at different sections on (a) 2-inch Si wafer; and (b) 4-inch Si wafer

The uniform appearance of the (100) peak with relatively consistent intensity and position across all measured spots suggests excellent crystalline alignment and uniformity of the AlN thin film as shown in magnified XRD pattern of AlN across 2-inch Si wafer in Fig. 4. This implies that the deposition process maintained good control over crystal orientation and film structure, regardless of the position on the wafer surface. Moreover, the sharpness and intensity of the peaks indicate that the films possess high crystallinity with minimal structural defects. The absence of other major peaks implies a strong preferential orientation with minimal presence of other crystalline planes, further supporting the conclusion that the film is either monocrystalline or highly textured along the (100) direction.

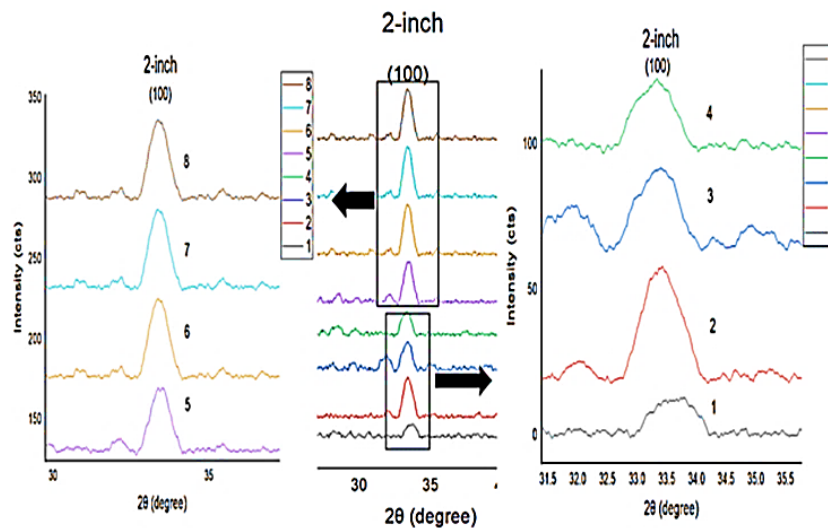


Fig. 4 Magnified XRD pattern of AlN on 2-inch Si wafer at section 1 to 8

The magnified XRD pattern of the AlN across the 4-inch Si wafer (Fig. 5) shows the regular (100) peak at all 16 sections. However, its intensity exhibits significant variation among them. The inset image illustrates how the yellow-marked spots, especially those along the wafer's borders (positions 1, 4, 5, 9, 13, and 16), have lower peak intensities of (100) plane than those in the centre. On the other hand, sections in the centre of the wafer show stronger and sharper (100) peak, which means that crystalline quality and homogeneity are better in the central areas. This spatial variation in XRD intensity is likely attributed to non-uniform temperature distribution, precursor flow, or stress relaxation effects during the deposition process, which are more prominent over larger substrates. The results indicate that while AlN growth maintains the (100) orientation across the entire 4-inch wafer, the crystallinity and texture are less uniform near the edges.

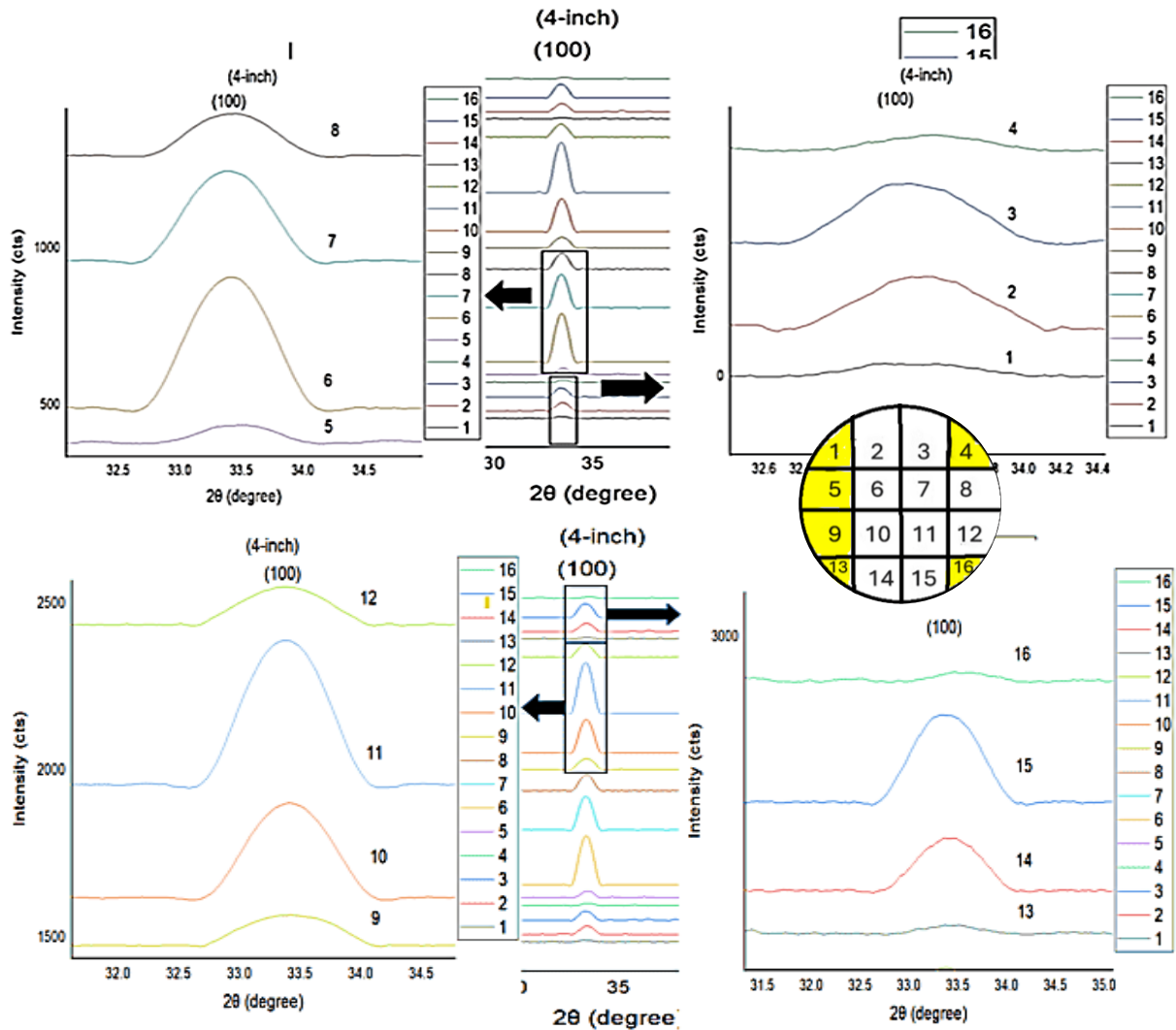


Fig. 5 Magnified XRD pattern of AlN on 4-inch Si wafer at section 1 to 16

Variations in plasma density, especially near the periphery of the deposition chamber, can lead to inconsistent energy and material delivery during film growth. Additionally, shadowing effects, where the edge of the substrate receives less uniform deposition due to geometry and angular distribution of the sputtered species can further impact film thickness and quality. Moreover, the target-to-substrate distance plays a critical role as for larger wafers, regions farther from the centreline of the sputtering source may receive reduced or angled flux, resulting in a non-uniform coating. These observations are consistent with previous reports on thin film deposition using physical vapor deposition (PVD) techniques [27][28]. The variation between the substrate size (4-inch) and the sputtering target diameter (3-inch Al target) could increase the uneven distribution of sputtered atoms, hence influencing film formation at the outermost edges.

3.2 AlN Thin Film Thickness Distribution

The XRD measurement reveals variations in crystal orientation intensity, especially at the edges of the 4-inch wafer, necessitating further assessment of thickness uniformity and surface morphology. In order to determine whether comparable non-uniform patterns are seen throughout the wafer surface and to aid in the comprehension of potential deposition-related reasons, a thorough examination of the thickness distribution is provided. Tape masking was used to create a step edge on the thin film, which is essential for thickness measurement using the surface profilometer method [29]. Fig. 6 shows the actual as-deposited AlN thin films on both wafers, along with schematic drawings of the tape masking applied to the 2-inch and 4-inch Si wafers prior to deposition for thickness analysis.

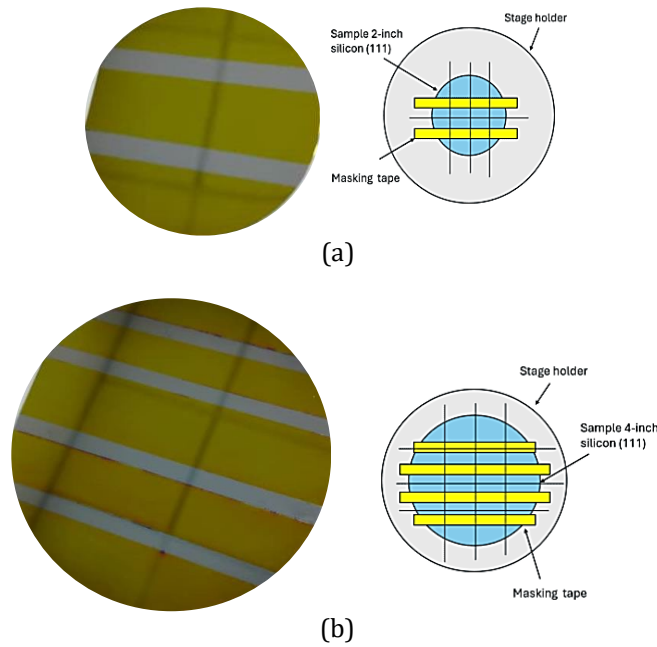
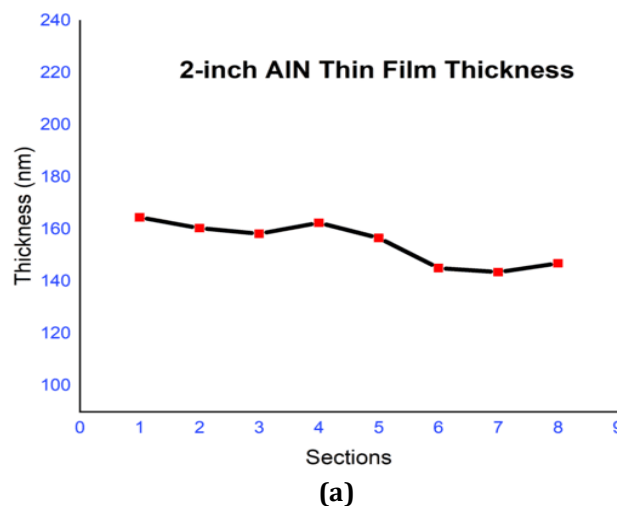


Fig. 6 AlN thin film on Si wafer with masking tape arrangement a) 2-inch Si wafer, and (b) 4-inch Si wafer

The thickness distribution of AlN thin films deposited on 2-inch and 4-inch Si wafers was assessed to determine the dimensional homogeneity of the coatings, as depicted in Fig. 7. Thickness uniformity is a crucial factor in thin film production, as it directly affects device performance, especially in optoelectronic and MEMS applications where constant dielectric or piezoelectric responses are vital. The film thickness on the 2-inch Si wafer varied from 133.38 nm to 168.45 nm across eight measured sites, yielding an average thickness of 154.28 nm and a standard deviation (σ) of 10.98 nm. The findings indicate a Coefficient of Variation (CV) of 7.12%. The CV was calculated using the following equation:

$$\text{Coefficient of Variation (CV)} = (\sigma / \mu) \times 100\% \tag{1}$$

Where σ is the standard deviation of the thickness measurements and μ is the mean (average) thickness. This relatively low CV indicates that the film is dimensionally homogeneous, with minimal thickness fluctuation across the entire wafer surface. On the other hand, the 4-inch Si wafer demonstrated a wider thickness distribution, spanning from 134.00 nm to 188.28 nm, with a mean thickness of 168.68 nm and a standard deviation of 13.74 nm, resulting in a coefficient of variation of 8.15%. The increased variation relative to the 2-inch wafer suggests a little less uniform thickness, particularly in the outside edges of the wafer, although it still below the 10% threshold. The trend lines in Fig. 7(a) and Fig. 7(b) reinforces these findings. The 2-inch wafer plot shows a relatively flat profile, with only minor fluctuations across all eight sections.



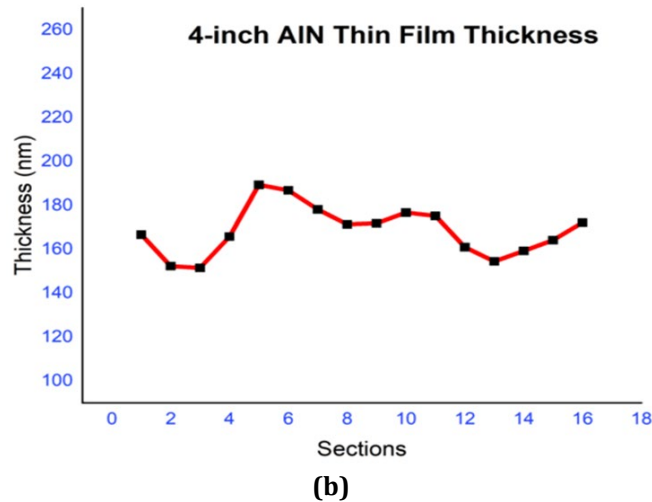


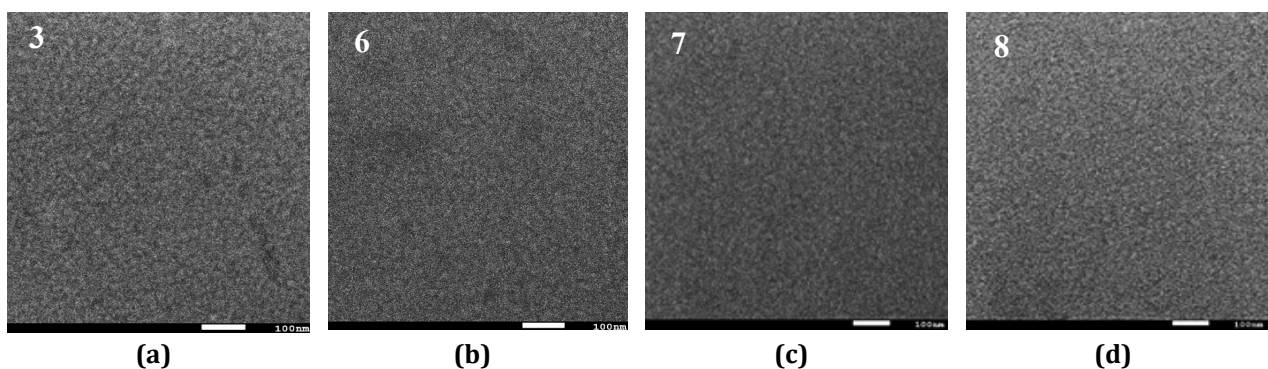
Fig. 7 AlN thickness distribution (a) 2-inch Si wafer; (b) 4-inch Si wafer

In contrast, the 4-inch wafer plot displays more pronounced variation, especially at sections located near the outer regions of the wafer. However, it is noteworthy that in the central region of the 4-inch wafer, the thickness values remain relatively consistent, closely resembling the uniform profile of the 2-inch wafer. This suggests that the deposition process provides good material distribution near the centre of the substrate, regardless of size. The increased deviation observed in the 4-inch wafer is primarily associated with the peripheral areas, where reduced material flux, angular distribution effects, and plasma density gradients become more significant.

These findings correlate with the XRD results, where weaker crystalline orientation was observed at the wafer edges, supporting the hypothesis that non-uniform material distribution occurred during deposition. The increased deviation in the 4-inch wafer is likely due to limitations in target size, angular flux distribution, and edge shadowing effects, which become more prominent over larger substrates. These factors can lead to non-uniform deposition rates, thereby affecting both the thickness and crystalline structure of the films.

3.3 Morphological of AlN Thin Film

Fig. 8 shows FESEM images of AlN thin films deposited on a 2-inch Si wafer at four positions: section 3 (top-central), section 6 (centre), section 7 (bottom-central), and section 8 (right-central). The corresponding spatial locations are mapped on the wafer in Fig. 8(e). These images were captured to assess the surface morphology uniformity of the AlN thin film across the wafer. The FESEM images reveal uniform surface features at all four locations, with consistently fine-grained and densely packed structures. No significant morphological differences are observed between the central and peripheral regions, indicating that the deposition process achieved stable and homogeneous film growth across the entire 2-inch wafer. The film appears smooth and well-covered, with no noticeable signs of agglomeration, surface cracking, or uneven grain formation.



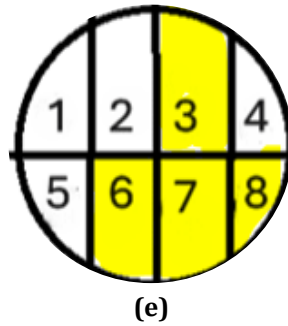


Fig. 8 FESEM mages of the surface morphology of AlN thin films deposited on a 2-inch Si wafer at four different sections: (a) section 3; (b) section 6; (c) section 7; and (d) section 8. The corresponding spatial locations are mapped on the wafer in (e)

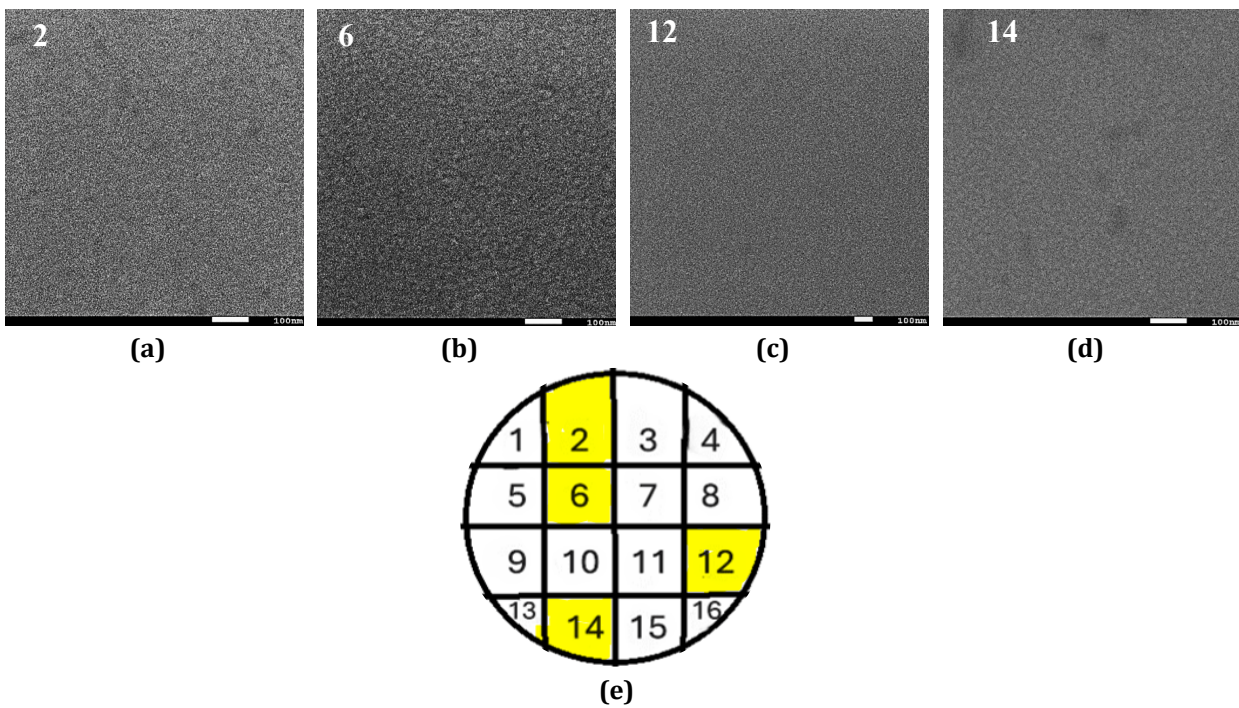


Fig. 9 FESEM mages of the surface morphology of AlN thin films deposited on a 4-inch Si wafer at four different sections: (a) section 2; (b) section 6; (c) section 12; and (d) section 14. The corresponding spatial locations are mapped on the wafer in (e)

This high degree of surface uniformity is in excellent agreement with the XRD results, which showed consistent (100) peak intensities across all positions, and with the thickness measurements that recorded a low coefficient of variation (CV) of 7.12%. The uniformity in surface morphology confirms that the smaller wafer size allowed for more consistent plasma exposure, even material distribution, and minimized edge effects during sputtering. For the AlN thin film across 4-inch Si wafer, Fig. 9 presents FESEM images of AlN thin films deposited at four distinct positions: section 2 (top-central), section 6 (centre), section 12 (mid-right), and section 14 (lower-central). The corresponding spatial locations are mapped in Fig. 11(e). At the centre of the wafer (section 6), the surface exhibits a dense and uniform grain structure, suggesting well-ordered film growth with consistent nucleation across the region. This morphology correlates well with previous XRD and thickness results, which also demonstrated high crystallinity and low variation in the central area. Moving outward to intermediate regions such as positions 2, 12, and 14, the surface remains relatively homogeneous but with small and less compact grain structures compared to the centre. This may indicate mild variations in deposition conditions due to reduced material flux or localized changes in plasma density as the distance from the target increases. The combined results from XRD, thickness, and FESEM analyses clearly demonstrate that the 2-inch wafer offers superior uniformity in terms of crystal orientation, film thickness, and surface morphology. In contrast, the 4-inch wafer,

although maintaining acceptable quality, experiences slight degradation in uniformity at the wafer edges due to scale-up challenges.

3.4 Factors Influencing AlN Thin Film Uniformity

In this study, a 3-inch Al target was used for sputtering on both 2-inch and 4-inch wafers. While this setup is sufficient for full coverage and uniform distribution on the 2-inch wafer, it presents limitations when scaled up to a 4-inch substrate. The sputtered flux from a smaller target tends to be concentrated near the centre of the wafer, with reduced deposition rates and angular incidence at the outer regions. Larger targets generally improve thickness uniformity across the substrate, especially as the target-substrate distance increases. Larger targets generally provide better uniformity, as the wider erosion area helps reduce particle overlap at the substrate centre, resulting in a more even film distribution [30][31]. This mismatch in coverage directly contributes to the variation in both thickness and crystalline orientation seen in the 4-inch wafer. Another contributing factor is the plasma density distribution within the sputtering chamber. In planar magnetron sputtering systems, the plasma density is typically highest directly above the target centre, decreasing toward the edges. As wafer size increases, more of the substrate surface lies in these lower-density regions, affecting energy delivery, adatom mobility, and film growth kinetics [31]–[33].

As shown in Fig. 10, the central regions of both wafer sizes, where plasma density is relatively high and sputtered atom flux is most concentrated, adatoms receive sufficient energy to migrate and reorganize into well-ordered crystalline domains. This leads to smooth surface morphology, strong (100) XRD peaks, and uniform film thickness. However, in the outer regions of the 4-inch wafer, where plasma density and ion energy decrease, adatom mobility becomes limited. As a result, adatoms are more likely to stick at their landing sites without sufficient diffusion, leading to defective grain growth, increased roughness, and inconsistent thickness.

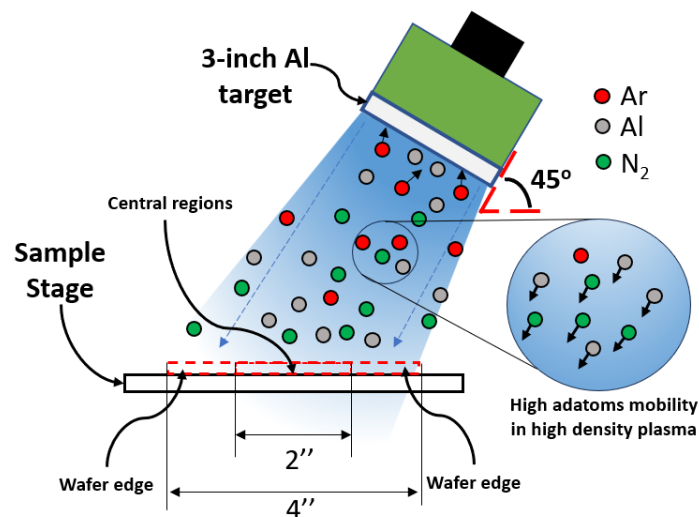


Fig. 10 Schematic representation of plasma species distribution and adatom mobility during AlN thin film deposition using a 3-inch Al target at a 45° oblique angle

4. Conclusion

This study compared the uniformity of AlN thin films deposited on 2-inch and 4-inch Si (111) wafers using RF magnetron sputtering with substrate rotation. The 2-inch wafer showed excellent uniformity in crystal orientation, thickness, and surface morphology. In contrast, the 4-inch wafer exhibited slight non-uniformities, especially at the edges, including reduced crystalline quality and increased thickness variation. These differences are mainly attributed to lower plasma density and reduced adatom mobility at the wafer periphery, as well as the mismatch between the 4-inch wafer and the 3-inch sputtering target. Although substrate rotation helped improve overall uniformity, it was not sufficient to fully compensate for the limited coverage and energy flux at the edges. While both CV values slightly exceed the ideal threshold of 5% typically required for active AlN layers, the films remain within acceptable limits for use as buffer layers, which are generally more tolerant to thickness variation. The uniform central region and overall crystalline orientation make the films promising for such applications. Under the current deposition arrangement, the 2-inch wafer showed more consistent film quality overall. Additional improvements, including employing a larger target or improving plasma distribution, might be necessary to increase uniformity on larger wafers.

Acknowledgement

This research was supported by the Malaysia Ministry of Science, Technology and Innovation (MOSTI) under the project "High Efficiency High Electron Mobility Transistor (HEMT) for Power Electronics Modules"(MOSTI005-2021SRF/SRF-APP PG1-P3). The project was a collaborative effort between Universiti Tun Hussein Onn Malaysia, Universiti Malaya, and MIMOS Berhad. This research also partially supported by Industrial Grant M177 at Universiti Tun Hussein Onn Malaysia.

Conflict of Interest

Authors declare that there is no conflict of interests regarding the publication of the paper.

Author Contribution

The authors confirm contribution to the paper as follows: **study conception and design:** Zulkifli Azman, Falah Abid Mohammad Shuhaili, Nafarizal Nayan, Mohd Rofei Mat Hussin; **data collection:** Falah Abid Mohammad Shuhaili, Zulkifli Azman; **analysis and interpretation of results:** Zulkifli Azman, Ahmad Shuhaimi Abu Bakar; **draft manuscript preparation:** Zulkifli Azman, Falah Abid Mohammad Shuhaili, Jahanzeb Khan, Nafarizal Nayan. All authors reviewed the results and approved the final version of the manuscript.

References

- [1] Z. Cheng *et al.*, "Experimental observation of high intrinsic thermal conductivity of AlN," *Phys. Rev. Mater.*, vol. 4, no. 4, p. 44602, 2020.
- [2] R. Yu *et al.*, "Ultrawide-bandgap semiconductor AlN crystals: growth and applications," *J. Mater. Chem. C*, vol. 9, no. 6, pp. 1852–1873, 2021.
- [3] M. Lee *et al.*, "Nanovoid-driven highly crystalline aluminum nitride and its application in solar-blind UV photodetectors," *J. Mater. Chem. C*, vol. 8, no. 41, pp. 14431–14438, 2020.
- [4] A. S. Bakri *et al.*, "Fabrication of w-AlN Thin Films using Tilted Sputter Target and Unrotated Substrate Holder," *Int. J. Integr. Eng.*, vol. 12, no. 4, pp. 50–56, 2020.
- [5] P. Shao *et al.*, "Step-flow growth of Al droplet free AlN epilayers grown by plasma assisted molecular beam epitaxy," *J. Phys. D. Appl. Phys.*, vol. 55, no. 36, p. 364002, 2022, doi: 10.1088/1361-6463/ac79dd.
- [6] A. Kakanakova-Georgieva *et al.*, "MOCVD of AlN on epitaxial graphene at extreme temperatures," *CrystEngComm*, vol. 23, no. 2, pp. 385–390, 2021, doi: 10.1039/d0ce01426e.
- [7] A. Iqbal and F. Mohd-yasin, "Reactive Sputtering of Aluminum Nitride (002) Thin Films for Piezoelectric Applications : A Review," no. 002, pp. 1–21, 2018, doi: 10.3390/s18061797.
- [8] D. L. Ma *et al.*, "Optimal target sputtering mode for aluminum nitride thin film deposition by high power pulsed magnetron sputtering," *Vacuum*, vol. 160, no. May 2018, pp. 410–417, 2019, doi: 10.1016/j.vacuum.2018.11.058.
- [9] S. Hussain *et al.*, "Photoluminescence Comparison of Different Substrates on AlN: Cr Thin Films for Optoelectronic Devices," *Adv. Sci. Technol.*, vol. 119, pp. 19–25, 2022, doi: 10.4028/p-1265j6.
- [10] E. Wang, H. Zhang, X. Xie, L. Xie, L. Bian, and G. Chen, "AlN Thin Films Grown on Different Substrates by Metal Nitride Vapor Phase Epitaxy," *Cryst. Res. Technol.*, vol. 58, 2023, doi: 10.1002/crat.202200196.
- [11] S. Liu, Y. Li, J. Tao, R. Tang, and X. Zheng, "Structural, Surface, and Optical Properties of AlN Thin Films Grown on Different Substrates by PEALD," 2023, [Online]. Available: <https://consensus.app/papers/structural-surface-and-optical-properties-of-aln-thin-zheng-tang/47421b772f7355a2a7a8f1542a13e176/>
- [12] Q. X. Guo, T. Tanaka, M. Nishio, and H. Ogawa, "Growth properties of AlN films on sapphire substrates by reactive sputtering," *Vacuum*, vol. 80, no. 7, pp. 716–718, 2006.
- [13] A. M. Cardenas-Valencia, S. Onishi, and B. Rossie, "Single-crystalline AlN growth on sapphire using physical vapor deposition," *Phys. Lett. A*, vol. 375, no. 6, pp. 1000–1004, 2011.
- [14] C. Duquenne, M.-P. Besland, P. Y. Tessier, E. Gautron, Y. Scudeller, and D. Averty, "Thermal conductivity of aluminium nitride thin films prepared by reactive magnetron sputtering," *J. Phys. D. Appl. Phys.*, vol. 45, no. 1, p. 15301, 2011.
- [15] A. Pandey, S. Dutta, R. Prakash, R. Raman, A. K. Kapoor, and D. Kaur, "Growth and Comparison of Residual Stress of AlN Films on Silicon (100), (110) and (111) Substrates," *J. Electron. Mater.*, vol. 47, no. 2, pp. 1405–1413, 2018, doi: 10.1007/s11664-017-5924-8.

- [16] J. Yin *et al.*, "Optical and structural properties of AlN thin films deposited on different faces of sapphire substrates," *Semicond. Sci. Technol.*, vol. 36, 2021, doi: 10.1088/1361-6641/abe3c5.
- [17] M. K. Sandager, C. Kjelde, and V. Popok, "Growth of Thin AlN Films on Si Wafers by Reactive Magnetron Sputtering: Role of Processing Pressure, Magnetron Power and Nitrogen/Argon Gas Flow Ratio," *Crystals*, vol. 12, no. 10. 2022. doi: 10.3390/cryst12101379.
- [18] S. A. B. Abdullah *et al.*, "Fabrication of uniform aluminium nitrate thin film on 2-inch silicon substrate," in *2023 IEEE International Conference on Sensors and Nanotechnology (SENNANO)*, IEEE, 2023, pp. 85–88.
- [19] A. Le Febvrier, L. Landälv, T. Liersch, D. Sandmark, P. Sandström, and P. Eklund, "An upgraded ultra-high vacuum magnetron-sputtering system for high-versatility and software-controlled deposition," *Vacuum*, vol. 187, p. 110137, 2021.
- [20] Z. Cheng *et al.*, "Deposition and structural investigation of uniform AlN (100) films at wafer scale through RF magnetron sputtering," *Ceram. Int.*, vol. 50, no. 16, pp. 28601–28608, 2024.
- [21] Q. Qin *et al.*, "Investigating the physical mechanism of ion-slicing in AlN and hetero-integrating AlN thin film on Si (100) substrate," *Mater. Sci. Semicond. Process.*, vol. 176, p. 108346, 2024.
- [22] M. Aqib, S. Pouladi, M. Moradnia, R. P. R. Kumar, N.-I. Kim, and J.-H. Ryou, "Strain accumulation and relaxation on crack formation in epitaxial AlN film on Si (111) substrate," *Appl. Phys. Lett.*, vol. 124, no. 4, 2024.
- [23] F. K. Mohammed, A. Ramizy, N. M. Ahmed, F. K. Yam, Z. Hassan, and K. P. Beh, "Characteristics of aluminium nitride thin film prepared by pulse laser deposition with varying laser pulses," *Opt. Mater. (Amst.)*, vol. 153, p. 115622, 2024.
- [24] X. Cui *et al.*, "Unprecedented atomic surface of silicon induced by environmentally friendly chemical mechanical polishing," *Nanoscale*, vol. 15, no. 21, pp. 9304–9314, 2023.
- [25] Z. Cheng *et al.*, "Thermal Transport across Ion-Cut Monocrystalline β -Ga₂O₃ Thin Films and Bonded β -Ga₂O₃-SiC Interfaces," 2020.
- [26] Z. Azman *et al.*, "Investigating Crystallography and Thickness Distribution of Aluminium Nitride Thin Films Prepared by Magnetron Sputtering on Silicon Wafer," in *2024 IEEE 40th International Electronics Manufacturing Technology (IEMT)*, 2024, pp. 1–5. doi: 10.1109/IEMT61324.2024.10875098.
- [27] N. On *et al.*, "Boosting carrier mobility and stability in indium-zinc-tin oxide thin-film transistors through controlled crystallization," *Sci. Rep.*, vol. 10, no. 1, p. 18868, 2020.
- [28] K. Kandpal, J. Singh, N. Gupta, and C. Shekhar, "Effect of thickness on the properties of ZnO thin films prepared by reactive RF sputtering," *J. Mater. Sci. Mater. Electron.*, vol. 29, pp. 14501–14507, 2018.
- [29] Z. Hong, "Optical interferometry for thickness measurement of opaque thin films and the influence of step fabrication," *Vacuum*, 2007, [Online]. Available: <https://consensus.app/papers/optical-interferometry-for-thickness-measurement-of-hong/7ea28c8e83a55722b3d5464d3b6a7451/>
- [30] G. Zhu, Y. Yang, B. Xiao, and Z. Gan, "Evolution Mechanism of Sputtered Film Uniformity with the Erosion Groove Size: Integrated Simulation and Experiment," *Molecules*, vol. 28, no. 22, p. 7660, 2023.
- [31] Z. Cheng *et al.*, "Realizing Ultrauniform Films at Wafer Scale through the Magnetron Sputtering Method," *Cryst. Growth & Des.*, 2023, doi: 10.1021/acs.cgd.3c01048.
- [32] J. Li, Q. An, and H. Fang, "Monte Carlo simulation of deposition uniformity in the triple-target magnetron co-sputtering system," *Appl. Surf. Sci.*, 2023, doi: 10.1016/j.apsusc.2023.158914.
- [33] G. Zhu, B. Xiao, G. Chen, and Z. Gan, "Study on the Deposition Uniformity of Triple-Target Magnetron Co-Sputtering System: Numerical Simulation and Experiment," *Materials (Basel)*, vol. 15, 2022, doi: 10.3390/ma15217770.